

Simultaneous Determination of m-Trihydroxybenzene and p-Nitrophenol at Glassy Carbon Electrode Modified with Graphene Oxide

Hongying Li^{1,2}, Xueliang Wang², Tao Wang², Zhaoxia Wang², Wei Zhao^{1,*}

¹ School of Chemical Engineering, China University of Mining and Technology, Xuzhou, 221116, Jiangsu, P.R.China.

² Department of Chemistry and Chemical Engineering, Heze University, Heze, 274015, Shandong, P. R. China.

*E-mail: hxxlhy@163.com

Received: 21 August 2016 / *Accepted:* 28 September 2016 / *Published:* 10 November 2016

A modified electrode was fabricated by casting graphene oxide (GO) suspension onto the surface of active glassy carbon electrode (GCE), and it can significantly enhanced the oxidation peak currents of m-trihydroxybenzene (m-THB) and p-nitrophenol (p-NP). Based on this, a sensitive analytical method towards their simultaneous determination was established. Many influencing factors such as the type of electrolyte, acidity, scan rates and concentrations were explored. Under the optimal experimental conditions, the oxidation peak currents of m-THB and p-NP were linearly increased with their concentrations ranging from 9 to 100 μM , with the detection limits both of 1 μM . Comparing with other reported methods, this sensor showed wider linear range and lower detection limit. In addition, the proposed method was successfully used to analysis of real environmental water samples with satisfactory recoveries, which verified the practicability of the sensor.

Keywords: m-trihydroxybenzene, p-nitrophenol, graphene oxide, modified electrode

1. INTRODUCTION

m-Trihydroxybenzene (m-THB), also called phloroglucinol, is a kind of important phenolic compound, and widely used in many ways, such as used as a biological reagent to make dyes, drugs, resin, used as smooth muscle relaxant, and used to test the vanilla essence, wood, etc. However, if it is released into environment in the process of preparation or use, then, will cause some harm to environment. Also, it can cause humans acute poisoning: vomiting, hypothermia, weakness, ataxia, cyanosis, coma, asphyxia, and even death. Long term contact can cause anemia, jaundice, sensitization to the skin, eczema. Therefore, it is very important for environmental monitoring and clinical treatment

to set up an appropriate method to accurately and sensitively detect its concentration. Until today, there are some analytical methods reported for its determination, such as Liquid Chromatography-tandem Mass Spectrometry,[1] High Performance Liquid Chromatography (HPLC),[2] Ion Chromatography with Chemiluminescence,[3] Gas Chromatography Mass Spectrometry (GC-MS),[4] however, these methods are time consuming and high cost, thus, developing a simple and fast detection method is very expected.

p-Nitrophenol (p-NP), is an important chemical intermediate, and widely used to fabricate many fine chemicals, such as pesticides, pharmaceuticals, dyes and so on, also can be used as leather preservative and acid base indicator. However, it has toxic effects on humans, animals and plants even at very low concentration, and has been added into the U.S. Environmental Protection Agency List of Priority Pollutants.[5] Hence, the analysis of p-NP is very importance for the environmental control. Many techniques were developed for the determination of p-NP, such as molecularly imprinted,[6] liquid chromatography,[7, 8] UV-vis spectrophotometry,[9] chemiluminescence,[10] and so on. Most of these methods required complex sample preparation process and skilled operator, which limited their use. Being an electro-active substance, p-NP can be detected by electrochemical method. Additionally, electrochemical methods have many advantages of low cost, fast response, simple operation and sensitive, comparing with other methods mentioned above, therefore, it developed rapidly in recent years, and many literatures were reported about the determination of p-NP by various electrochemical techniques.[11, 12, 13-25] In order to enhance the sensitive of determination, many materials were employed to modify electrodes, such as nanoparticles,[13, 14] polymer film,[15-18] carbon nanotube,[19] graphene based materials,[20-24] mesoporous carbon,[25] and other compound materials.[26, 27] Among all modified materials, graphene was one of the most frequently used materials due to the virtues of good chemical stability, outstanding electrical conductivity, excellent physicochemical, mechanical and electronic properties.[28] Graphene oxide (GO) is the product of graphite powder through chemical oxidation and stripping, and has a single atomic layer with more functional groups containing oxygen, which make it has more active nature than graphene, and shows better catalytic effect. Feng Gao and co-workers used it to modify electrode, and greatly enhanced the electrochemical redox current of dopamine, thus achieved the highly sensitive and selective detection of dopamine in the presence of ascorbic acid.[29] In another paper, they used it as the multi-site platform for probe DNA immobilization, and obtained the remarkable response signal, and fabricated a sensitive DNA biosensor. [30] Zuo and co-workers demonstrated graphene oxide could facilitate the electron transfer of several metalloproteins at electrode surfaces.[31]

In this work, GO exhibited good catalytic activity to the oxidation reaction of m-THB and p-NP, and significantly enhanced their oxidation peak currents, based on this, an analysis method for simultaneous determination of m-THB and p-NP at GO modified electrode was set up.

2. EXPERIMENTAL

2.1 Chemicals and instrument

m-Trihydroxybenzene was purchased from Shanghai Macklin Biochemical Co.,Ltd (China), p-NP was purchased from Tianjin Kemiou Chemical Reagent Co., Ltd (China). GO was obtained from

JCNANO Co., Ltd (Nanjing, China). N, N- Dimethylformamide (DMF) was purchased from Tianjin FuYu Fine Chemical Co., Ltd (China). 1-(3-dimethylaminopropyl)-3-ethylcarbodiimide hydrochloride (EDC) and N-Hydroxy succinimide (NHS) were obtained from Shanghai Aladdin Reagent Co., Ltd (China). All other reagents were analytical reagent grade and used as received. Triple distilled water was used throughout all experiments.

CHI 920C electrochemical workstation (Chenhua, Shanghai) with a conventional three-electrode cell of glass carbon electrode (GCE) or modified electrode working electrode, a platinum foil counter electrode, and a saturated calomel reference electrode, was employed for all electrochemical determination.

2.2 Experimental method

0.1 M m-THB and 0.1 M p-NP stock solution were obtained by dissolving 1.26 g of m-THB or 1.39 g of p-NP into 100 mL absolute alcohol. 1.0 mg/mL GO suspension was prepared by dispersing 1.0 mg GO into 1.0 mL DMF with ultrasonication for 6 h. 0.1 M acetate buffer solution (ABS) with different pHs were prepared by adjusting 0.1 M HAc (containing 0.1 M KCl) and 0.1 M NaAc (containing 0.1 M KCl). 0.1 M phosphate buffer solution (PBS) was prepared by adjusting 0.1 M NaH_2PO_4 (containing 0.1 M KCl) and 0.1 M Na_2HPO_4 (containing 0.1 M KCl). 0.1 M Tris(hydroxymethyl)aminomethane (Tris) (containing 0.1 M KCl) and 0.1 M HCl (containing 0.1 M KCl) were mixed to be 0.1 M Tris-HCl buffer solution.

Differential Pulse Voltammetry (DPV) was employed to the detection experiments, and the parameters were set as follows: increment of 0.01 V, amplitude of 0.05 V, pulse width of 0.2 s, pulse period of 0.5 s.

2.3 Preparation of modified electrode

The modification process was similar to that of reference 29. Before modification, GCE was polished on a chamois leather with 50 nm alumina slurry, rinsed successively with diluted acetone, absolute ethanol, and triple-distilled water in ultrasonic bath for 5 min, then oxidized at + 1.5 V for 15 s in an mixed solution containing 10% HNO_3 and 2.5% $\text{K}_2\text{Cr}_2\text{O}_7$ to generate some active groups.[32] 10 μL PBS containing 8 mM NHS and 5 mM EDC was cast to the oxidized GCE surface for 5 h, and a rubber cap fitted to prevent evaporation. Finally, 6 μL GO suspension was cast on the active GCE, and allowed to air dry. Before use, the modified GCE was rinsed with triple-distilled water carefully to remove the loosely attached GO, then dried naturally and denoted as GO/GCE.

3. RESULTS AND DISCUSSION

3.1 Characterization of GO/GCE

Bare GCE and GO/GCE was characterized by Cyclic Voltammetry (CV), the results showed in Figure 1. As 1.0 mM $[\text{Fe}(\text{CN})_6]^{3-/4-}$ (1:1) with 0.1 M KCl was electrochemical probe, a pair of well-

defined redox peaks corresponding to the electron transfer of $\text{Fe}^{\text{II}}/\text{Fe}^{\text{III}}$ couple was obtained at bare GCE (Figure 1A curve a). As GO/GCE used as working electrode, the redox peaks of $[\text{Fe}(\text{CN})_6]^{3-/4-}$ decrease obviously (Figure 1A curve b). On the contrary, when 1.0 mM $\text{Ru}(\text{NH}_3)_6]^{2+/3+}$ was used as electrochemical probe, the redox peak current of $\text{Ru}(\text{NH}_3)_6]^{2+/3+}$ on GO/GCE (Figure 1B curve b) was increased in comparison with those on bare GCE (Figure 1B curve a). These different changes can be ascribed to the negatively charged GO. As is known to all that GO contains rich $-\text{OH}$ and $-\text{COOH}$, and shows negative-charge characteristic, therefore, the electrode modified with GO will repel anionic species (for example, $[\text{Fe}(\text{CN})_6]^{3-/4-}$) through electrostatic repulsion while attract cationic species (such as, $\text{Ru}(\text{NH}_3)_6]^{2+/3+}$) via electrostatic attraction, so, the results in Figure 1 appeared, which exactly testified that GO had been immobilized onto GCE surface.

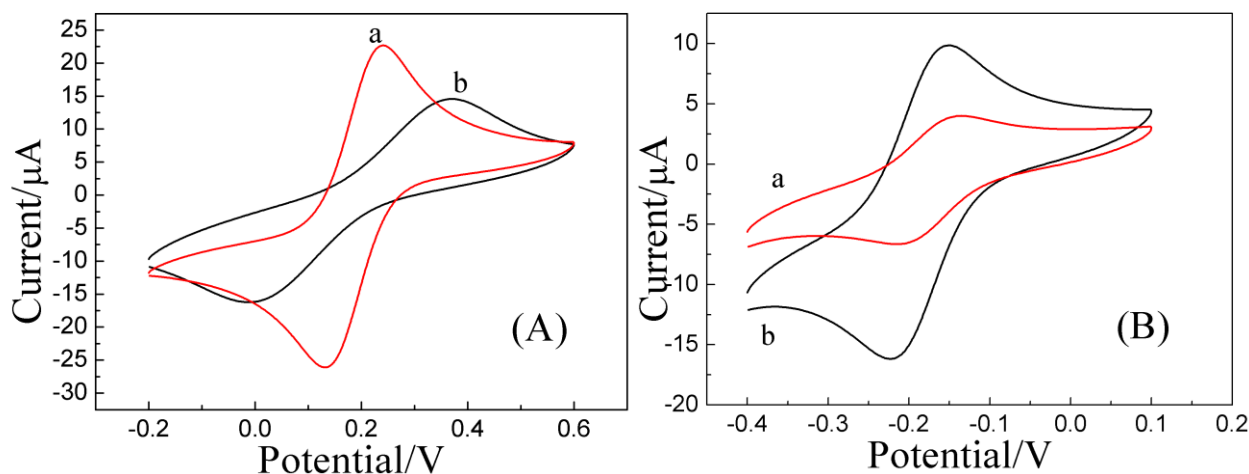


Figure 1. Cyclic voltammograms of 1.0 mM $[\text{Fe}(\text{CN})_6]^{3-/4-}$ (1:1) with 0.1 M KCl (A) and 1.0 mM $[\text{Ru}(\text{NH}_3)_6]^{3+}$ (B) at bare GCE (a) and GO/GCE (b).

3.2 Electrochemical oxidation of *m*-THB and *p*-NP at different electrodes

In order to investigate the electrochemical behaviour of *m*-THB and *p*-NP at different electrodes, CV was carried on in 30 μM *m*-THB and 30 μM *p*-NP in 0.1 M ABS of pH 4.0 with the potential ranging from -1.0 to +1.2 V, and the results showed in Figure 2. It can be seen from Figure 2 A that one oxidation peak at 0.72 V and one reduction peak at -0.66 V towards *m*-THB were observed at bare GCE (curve a). When GO/GCE was used as working electrode (curve b), oxidation peak current significantly enhanced, and the oxidation peak potential shifted positively to +0.77 V; reduction peak current had no obvious increase, and reduction peak potential shifted negatively to -0.73 V. As to *p*-NP (Figure 2 B), at bare GCE (curve a), one oxidation peak at +0.31 V and one reduction peak at -0.65 V were obtained. As GO/GCE used as working electrode, three peaks appeared: oxidation peak at +0.31 V shifted positively to +0.33 V, reduction peak at -0.65 V shifted negatively to -0.76 V, a new oxidation peak at +1.08 V was observed, and all peaks current increased obviously. There are three reasons can be used to explain the increase of peak current.: first, GO has high surface area and can enhance adsorption and fixing capability; second, GO has high conductivity and is conducive to the occurrence of oxidation reaction; third, GO has unoxidized aromatic rings with

rich delocalized π electrons, and have strong ability to interact with some substances containing special aromatic ring through π - π staking mode. [33-35] Both m-THB and p-NP have a special aromatic ring, therefore, the electron communication and interaction between two analytes and GO was further strengthened via π - π staking force, which can further increase their electrochemical response.

Comparing with those at bare GCE, all oxidation peaks potential shifted positively, and all reduction peaks potential shifted negatively at GO/GCE, which can be ascribed to the electrostatic repulsion between GO and the critical complex of their electrochemical reaction. GO shows negative-charge characteristic, and the critical complex of redox reaction between phenols and quinones are negatively charged aromatic [29] (the structures were shown in Figure 3), too, therefore, the electrostatic repulsion between them made the overpotential of electrochemical reaction increase, and caused the shift of peak potential.

In order to simultaneous determination of m-THB and p-NP in mixture solution, their reduction peaks were abandoned because that the similar peaks potential could not distinguish them. Two oxidation peaks of p-NP can be used to the simultaneous determination, however, the current of oxidation peak at + 1.08 V is larger than that of peak at + 0.33 V, in order to reduce detection limit, the former was chosen to the simultaneous determination. Thus, two oxidation peak at + 0.77 V of m-THB and + 1.08 V of p-NP were used in the following determination experiments.

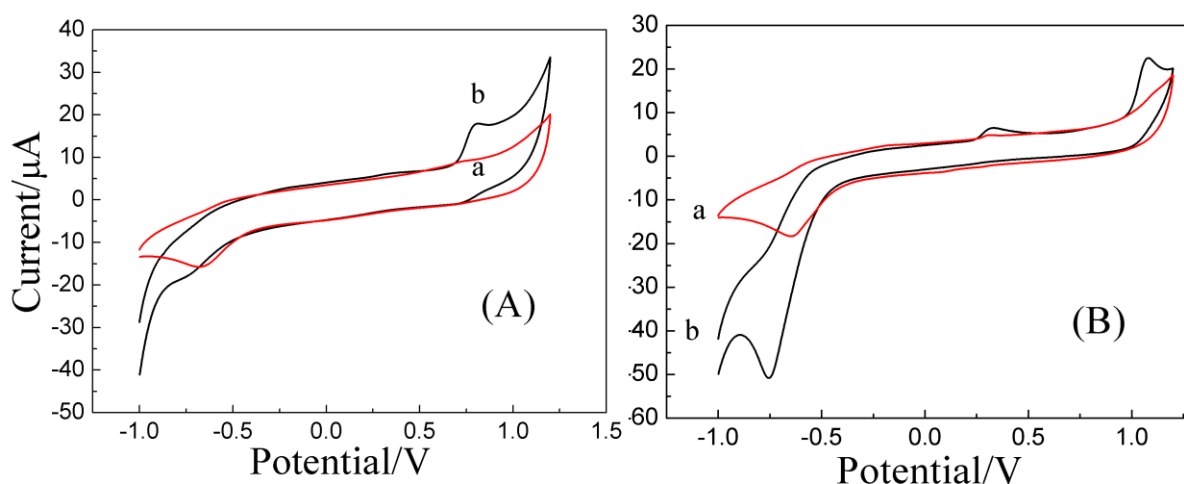


Figure 2. Cyclic voltammograms of 30 μ M m-THB (A) and 30 μ M p-NP (B) in 0.1 M ABS of pH 4.0 at bare GCE (a) and GO/GCE (b).

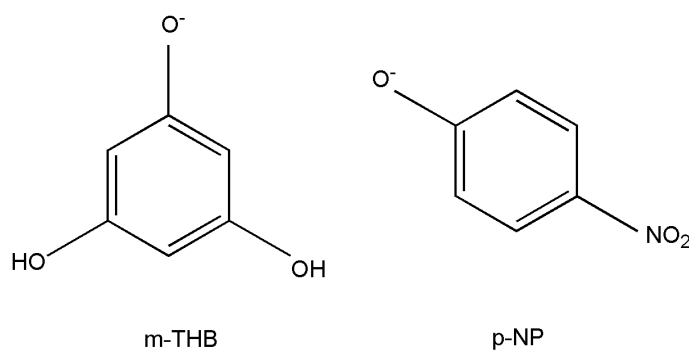


Figure 3. The structures of critical complex for m-THB and p-NP in electrochemical reaction.

3.3 The effect of supporting electrolyte

In order to find the appropriate supporting electrolyte for the determination of m-THB and p-NP, DPV was carried on in 20 μM m-THB and 20 μM p-NP in three base solutions at the same pH of 4.0, namely, 0.1 M Tris-HCl, 0.1 M PBS and 0.1 M ABS. It can be seen from Figure 4 that the baseline is too high to highlight the electrochemical signal of analytes in Tris-HCl (curve a), in addition, oxidation peak currents of m-THB and p-NP in ABS (curve c) were greater than those in PBS (curve b), and the shape of oxidation peaks were more symmetric, therefore, after synthetical consideration, ABS is more appropriate to be the supporting electrolyte, and used for the simultaneous determination of m-THB and p-NP.

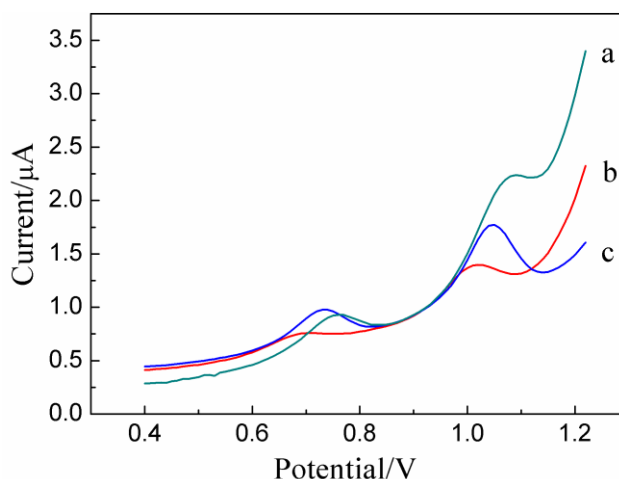


Figure 4. DPVs of 20 μM m-THB and 20 μM p-NP in 0.1 M Tris-HCl (a), 0.1 M PBS (b), and 0.1 mol L⁻¹ ABS (c) of pH 4.0 at GO/GCE.

3.4 The effect of pH

To investigate the effect of solution pH, DPV was performed to detect 20 μM m-THB and 20 μM p-NP in 0.1M ABS with different pHs (3.5 - 6.5) at GO/GCE, and the experimental results were shown in Figure 5, the oxidation peak currents of m-THB increased as pH increasing from 3.5 to 4.5, and reached the top at pH of 4.5, then decreased with pH further increasing, thus, the maximum oxidation peak current of m-THB was obtained at pH 4.5. However, the oxidation peak current of p-NP mainly decreased with the pH increasing from 3.5 to 6.0, and then slightly increased with pH further increasing, therefore, the maximum current was obtained at pH 3.5. Anyhow, considering of two kinds of substances, 4.0 was chosen as the optimum pH for the simultaneous determination of m-THB and p-NP.

The oxidation peak potentials of m-THB and p-NP shifted negatively with pH increasing from 3.5 to 6.5, indicating that their oxidation process involved proton transferring.

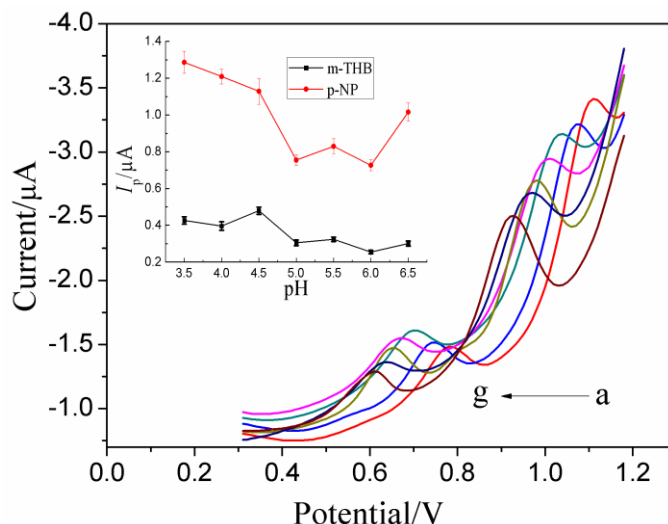


Figure 5. DPVs of 20 μM m-THB and 20 μM p-NP in 0.1 M ABS with different pHs (a-g: pH 3.5, 4.0, 4.5, 5.0, 5.5, 6.0, 6.5). Inset: the relationship of oxidation peak currents and pHs.

3.5 The effect of scan rate

To study the effect of scan rate, Linear Sweep Voltammetry (LSV) was performed in 80 μM m-THB and 80 μM p-NP at GO/GCE with different scan rates (10, 30, 50, 80, 110, 130 mV s^{-1}), and the results were shown in Figure 6. The oxidation peak currents of m-THB and p-NP linearly increased with the scan rate increasing, and the regression equations can be expressed as followings: I_p (μA) = $0.2726 (\pm 0.0103) v^{1/2} ((\text{mV s}^{-1})^{1/2}) - 0.1767 \pm 0.0847$, $R^2 = 0.9930$ for m-THB, and I_p (μA) = $0.3406 (\pm 0.0139) v^{1/2} ((\text{mV s}^{-1})^{1/2}) + 0.5926 \pm 0.1152$, $R^2 = 0.9917$ for p-NP, suggesting that the electrochemical oxidation of m-THB and p-NP at GO/GCE were diffusion-controlled processes.[36]

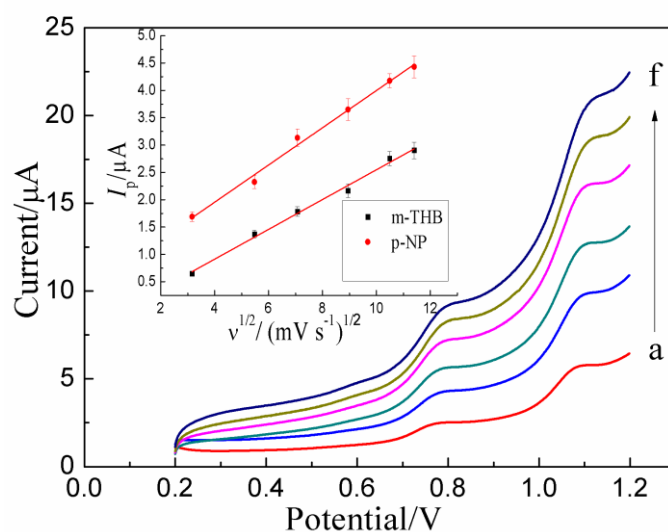


Figure 6. LSVs of 80 μM m-THB and 80 μM p-NP at GO/GCE with different scan rates (a-f: 10, 30, 50, 80, 110, 130 mV s^{-1}).

3.6 Respective determination of *m*-THB or *p*-NP

DPV was employed to respective determination of *m*-THB or *p*-NP in their mixture at GO/GCE under optimum conditions. First, keeping *p*-NP at constant concentration of 20 μM , changing *m*-THB concentration from 4 to 30 μM , experimental results showed the oxidation peak currents of *m*-THB were dependent on its concentrations (Figure 7 A), and the linear regression equation can be expressed as: $I_p (\mu\text{A}) = 0.0408 (\pm 0.0021) C_{m\text{-THB}} (\mu\text{M}) + 0.1195 \pm 0.0334$, $R^2 = 0.9871$, with the detection limit of 1 μM . The detection limit was obtained by continuously diluting *m*-THB solution until distinguishing the signal.

The similar experiment was performed for the respective determination of *p*-NP (Figure 7 B), keeping *m*-THB at 20 μM , and changing *p*-NP from 5 to 100 μM , the regression equation can be shown as: $I_p (\mu\text{A}) = 0.0296 (\pm 0.0016) C_{p\text{-NP}} (\mu\text{M}) + 0.3542 \pm 0.0855$, $R^2 = 0.9851$, with the detection limit of 1 μM .

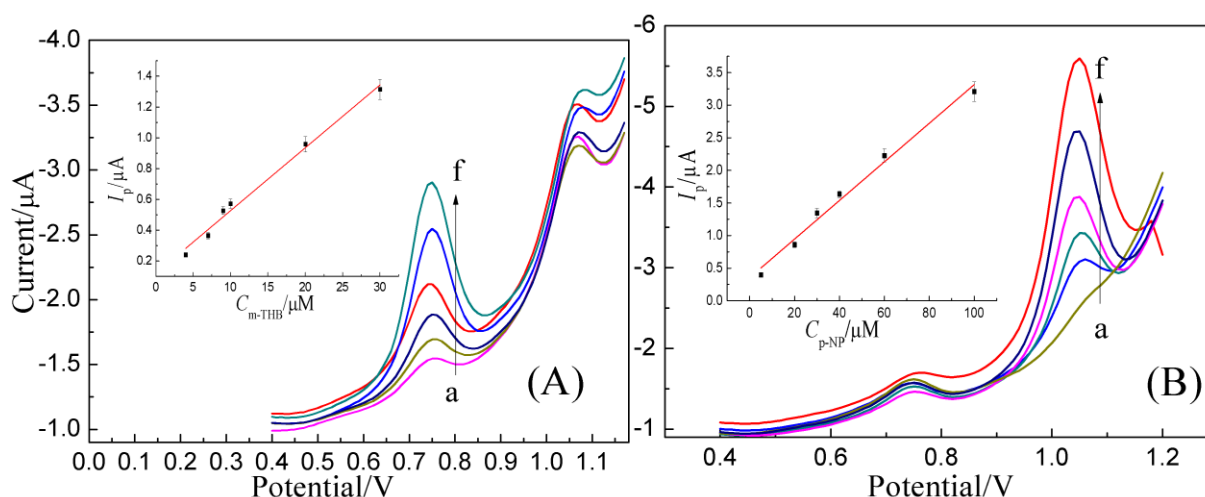


Figure 7. (A) DPVs of *m*-THB with different concentration (a-f: 4, 7, 9, 10, 20, 30 μM) and keeping *p*-NP of 20 μM at GO/GCE. Inset: the plot of I_p and $C_{m\text{-THB}}$. (B) DPVs of *p*-NP with different concentration (a-f: 5, 20, 30, 40, 60, 100 μM) and keeping *m*-THB of 20 μM at GO/GCE. Inset: the plot of I_p and $C_{p\text{-NP}}$.

3.7 Simultaneous determination of *m*-THB and *p*-NP

Under optimum conditions, the simultaneous determination of *m*-THB and *p*-NP was performed by DPV through continuously dilution of their equal concentration mixture, and the experimental results were shown in Figure 8, their oxidation peak current were both linearly dependent on their concentration ranging from 9 to 100 μM , and the corresponding calibration curve can be expressed as followings: $I_p (\mu\text{A}) = 0.0186 (\pm 0.0009) C_{m\text{-THB}} (\mu\text{M}) + 0.0231 \pm 0.0506$, $R^2 = 0.9897$ for *m*-THB; $I_p (\mu\text{A}) = 0.0258 (\pm 0.0013) C_{p\text{-NP}} (\mu\text{M}) + 0.0318 \pm 0.0793$, $R^2 = 0.9868$ for *p*-NP. In addition, the detection limits were obtained to be 1 μM both for *m*-THB and *p*-NP.

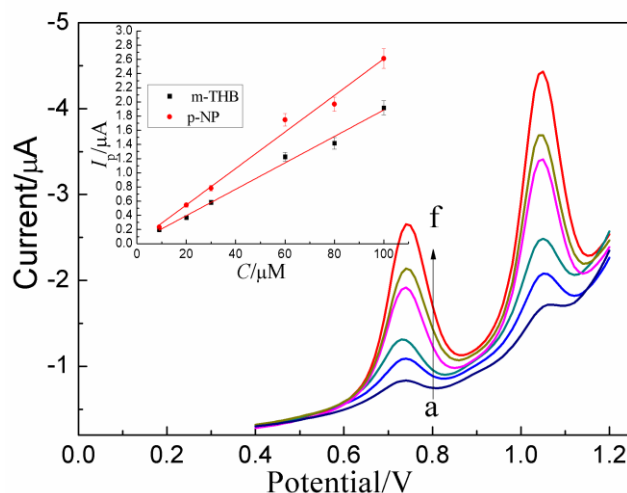


Figure 8. DPVs of m-THB and p-NP with various equal concentrations at GO/GCE. (a-f: 9, 20, 30, 60, 80, 100 μM)

The analytical performance comparison of the proposed sensor and other reported modified electrodes [27, 37-42] for detecting p-NP was summarized in Table 1. It is obvious that GO/GCE showed wider linear range and lower detection limit, which indicated its advantages of high adsorption capacity and good specificity for p-NP. So far, report on the electrochemical determination of m-THB were very few, thus the contrast is omitted.

Table 1. The analytical performance comparison of GO/GCE with other reported modified electrodes for the determination of p-NP.

Electrode	Linear range (μM)	Detection limit (μM)	Reference
Pt-Ag/AgCl electrode	100-3000	85	37
Nano-gold/GCE	10-1000	8	38
Nafion/GCE	20-230	17.1	39
Nanoporous Au electrode	1.8-72	-	40
Silver solid amalgam electrode	2-10	5.8	41
β -cyclodextrin/mesoporous silica electrode	2-14	0.1	27
β -cyclodextrin/ reduced graphene oxide electrode	7-70	0.36	42
GO/GCE	9-100	1	This work

3.8 Reproducibility, stability, interference

The reproducibility of this method was investigated via preparing three GO/GCEs at the same time, and using them to simultaneously detect m-THB and p-NP with equal concentration of 20 μM . Experimental results showed the relative standard deviations (RSD) were all $< 5.0\%$ for five determinations, suggesting good reproducibility of this sensor.

The stability of GO/GCE was studied by putting three modified electrodes into 4 °C refrigerator for 7, 14, 21 days, respectively, then using these electrodes to detect equal concentration of 20 μM of m-THB and p-NP (0.1M ABS of pH 4.0). Results showed the oxidation peak currents of m-THB and p-NP were 99%, 98%, 97% and 98%, 98% 97% of original current value, separately, indicating good stability of the proposed sensor.

The influence of some substances which may coexist in environmental water sample on m-THB and p-NP signals were investigated, and the results were listed in Table 2. It was found that Na⁺, Mg²⁺, Ca²⁺, K⁺, Cu²⁺, Cl⁻, SO₄²⁻, NO₃⁻ and NH₄⁺ almost have no effect on their detection, producing deviations of below 3%, but phenolic compounds such as bisphenol A, o-nitrophenol, m-nitrophenol and their derivatives, which have the similar oxidation potential to m-THB or p-NP, will interfere with their determination to a certain extent.

Table 2. The influence of interferences on the simultaneous determination of 20 μM m-THB and 20 μM p-NP (n=3).

Interferent	Concentration (μM)	Signal change (%)	
		m-THB	p-NP
Na ⁺	1000	+1.0	+0.6
Mg ²⁺	1000	-0.5	+1.4
K ⁺	1000	+1.6	+0.8
Ca ²⁺	1000	-0.7	+1.3
Cu ²⁺	1000	+2.4	+2.6
Cl ⁻	1000	-0.1	+0.4
SO ₄ ²⁻	1000	-1.4	-0.7
NO ₃ ⁻	1000	+0.4	+1.1
NH ₄ ⁺	1000	+1.2	-0.8
bisphenol A	100	+4.0	+3.5
o-nitrophenol	50	+2.1	+9.7
m-nitrophenol	50	+1.1	+10.2
2-aminaphenol	100	+5.8	+3.3
o-Chlorophenol	100	+3.6	+5.9
p-Chlorophenol	100	+3.5	+5.3

3.9 Real environmental water sample

To study the performance of modified electrode, real environmental water sample was detected by DPV at GO/GCE. Zhao-Wang River (a famous river in local district) water was diluted to 4 times of original volume with 0.1 M ABS (pH 4.0), then used as the real sample. From Figure 9 curve a, it was found that three oxidation peaks at 0.56, 0.77 and 0.92 V, respectively, were observed in the scan range of 0.2 to 1.2 V. In order to ascertain the ascription of oxidation peak, a certain amount of m-THB was added into the real sample, and the electrochemical signal was shown as Figure 9 curve b, the enhancement of current of peak at 0.77 V indicated the oxidation of m-THB. Similar experiment was performed via replacing m-THB by m-THB and p-NP, Figure 9 curve c exhibited that a new peak at

1.08 V corresponding to the oxidation of p-NP observed, illustrating the original water sample did not contain p-NP. The peaks at 0.56 and 0.92 V should correspond to the oxidation process of other substances. Standard addition method was carried on in this real water sample and tap water. The satisfactory recoveries (shown in Table 3) of 96.67% - 104.23% proved the valid and practicable of this method.

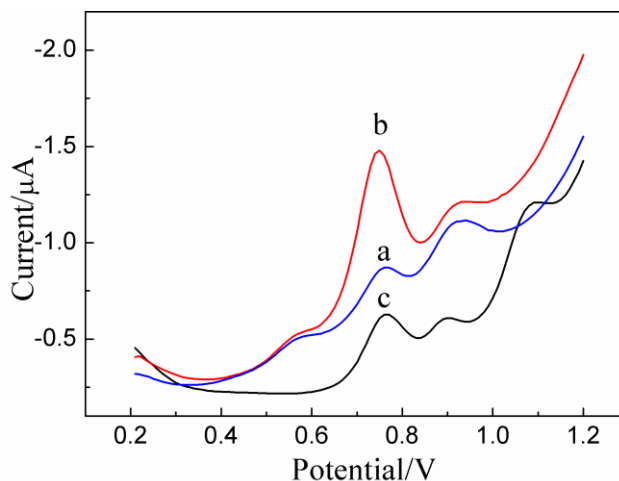


Figure 9. DPVs of Zhao-Wang River sample (a), Zhao-Wang River sample added with m-THB (b), Zhao-Wang River sample added with m-THB and p-NP (c).

Table 3. The results of standard addition method in real water sample (n=5).

Analyte	Water sample	Original (μM)	Added (μM)	Found (μM)	Recovery (%)	R.S.D (%)
m-THB	Zhao-Wang River water	8.00	10.00	18.02	100.11	3.8
		7.70	15.00	23.01	101.36	1.2
		7.90	20.00	26.97	96.67	2.3
	Tap water	0.00	10.00	10.03	100.30	1.3
		0.00	15.00	14.95	99.67	2.0
p-NP	Zhao-Wang River water	0.00	20.00	19.85	99.25	3.6
		0.00	30.00	31.30	104.23	4.1
		0.00	10.00	9.89	98.90	2.3
	Tap water	0.00	20.00	20.10	100.50	3.1
		0.00	30.00	30.12	100.40	2.0
		0.00	10.00	10.06	100.60	1.9

4. CONCLUSIONS

The proposed sensor was very convenient to fabricate, and successfully used to simultaneous determination of m-THB and p-NP with wider linear range and lower detection limit. The

determination of m-THB and p-NP in real environmental water sample obtained satisfactory recoveries, which proved the valid and practicable of GO/GCE. The advantages of high stability and good reproducibility of this sensor make it to be potential candidate for trace determination of m-THB and p-NP in the practical use.

ACKNOWLEDGEMENTS

This work was supported by Jiangsu Provincial Natural Science Foundation (Grant BK20151140), Shandong Province High School Science and Technology Planning Project (grant number J13LD51); Natural Science Foundation of Shandong Province, China (grant numbers BS2013HZ027, ZR2015BL014); the National Natural Science Foundation of China (grant number 21105023); and China Postdoctoral Science Foundation (grant number 2015M572039).

References

1. H. Kim and S. Han, *Chromatographia*, 57(2003)539.
2. H. Kim, H. Roh, H. Lee, S. Chung, S. Choi, K Lee and S. Han, *J Chromatogr B*, 792(2003)307.
3. H. Wu, M. Chen, D. Shou and Y. Zhu, *Chin J Anal Chem*, 40(2012)1747.
4. C. Lartigue-Mattei, C. Lauro-Marty, M. Bastde, J.A. Berger, J.L. Chabard, E. Goutay and J.M. Aiache, *J. Chromatogr*, 617(1993)140.
5. Toxic Substance Control Act, US Environmental Protection Agency, Washington, DC, 1979.
6. J. Luo, J. Cong, J. Liu and X. Liu, *Anal Chim Acta*, 864(2015)74.
7. X. Liu, Y. Ji, Y. Zhang, H. Zhang and M. Liu, *J Chromatogr A*, 1165(2007)10.
8. M. Mei, X. Huang, J. Yu and D. Yuan, *Talanta*, 134(2015)89.
9. M.I. Toral, A. Beattie, C. Santibañez and P. Richter, *Environ Monit Assess*, 76(2002)263.
10. J. Liu, H. Chen, Z. Lin and J.M. Lin, *Anal Chem*, 82(2010)7380.
11. M. Santhiago, C.S. Henry and L.T. Kubota, *Electrochim Acta*, 130(2014)771.
12. Y. Gu, Y. Zhang, F. Zhang, J. Wei, C. Wang, Y. Du and W. Ye, *Electrochim Acta*, 56(2010) 953.
13. P. Wang, J. Xiao, A. Liao, P. Li, M. Guo, Y. Xia, Z. Li, X. Jiang and W. Huang, *Electrochim Acta*, 176(2015)448.
14. H. Yin, Y. Zhou, S. Ai, X. Liu, L. Zhu and L. Lu, *Microchim Acta*, 169(2010)87.
15. T. Wei, X. Huang, Q. Zeng and L. Wang, *J Electroanal Chem*, 743(2015)105.
16. C. Yao, H. Sun, H. Fu and Z. Tan, *Electrochim Acta*, 156(2015)163.
17. Y. Zhang, L. Wu, W. Lei, X. Xia, M. Xia and Q. Hao, *Electrochim Acta*, 146(2014)568.
18. A.D. Arulraj, M. Vijayan and V. S. Vasantha, *Anal Chim Acta*, 899(2015)66.
19. H. Wu, L. Guo, J. Zhang, S. Miao, C. He, B. Wang, Y. Wu and Z. Chen, *Sensor Actuat B: Chem*, 230(2016)359.
20. R. Oliveira, N. Santos, L. Almeida Alves, K. Lima, L. Kubota, F. Damos and R. Silva Luz, *Sensor Actuat B: Chem*, 221(2015)740.
21. L. Yang, H. Zhao, Y. Li and C. Li, *Sensor Actuat B: Chem*, 207(2015)1.
22. N. Ikhsan, P. Rameshkumar and N. Huang, *Electrochim Acta*, 192(2016)392.
23. J. Li, D. Kuang, Y. Feng, F. Zhang, Z. Xu and M. Liu, *J. Hazard Mater*, 201–202(2012)250.
24. G. Bharath, R. Madhu, S. Chen, V. Veeramani, D. Mangalaraj and N. Ponpandian, *J Mater Chem A* 3(2015)15529.
25. T. Zhang, Q. Lang, D. Yang, L. Li, L. Zeng, C. Zheng, T. Li, M. Wei and A. Liu, *Electrochim Acta*, 106(2013)127.
26. P. Deng, Z. Xu, Y. Feng and J. Li, *Sensor Actuat B: Chem*, 168(2012)381.

27. X. Xu, Z. Liu, X. Zhang, S. Duan, S. Xu and C. Zhou, *Electrochim Acta*, 58(2011)142.
28. J. Hass, W. De Heer and E. Conrad, *J Phys: Condens Matter*, 20(2008)323202.
29. F. Gao, X. Cai, X. Wang, C. Gao, S. Liu, F. Gao and Q. Wang, *Sensor Actuat B: Chem*, 186(2013)380.
30. F. Gao, X. Cai, H. Tanaka, Q. Zhu, F. Gao and Q. Wang, *J Electrochem Soc*, 162(2015)B291.
31. X. Zuo, S. He, D. Li, C. Peng, Q. Huang, S. Song and C. Fan, *Langmuir*, 26(2010)1936.
32. G. Xu, K. Jiao, J. Fan and W. Sun, *Acta Chimica Slovaca*, 53(2006)486.
33. X. Zhang, Y. Feng, S. Tang and W. Feng, *Carbon*, 48(2010)211.
34. C. Zhang, L. Ren, X. Wang and T. Liu, *J Phys Chem C* 114(2010)11435.
35. W. Pu, L. Zhang and C. Huang, *Anal Methods*, 4(2012)1662.
36. J. Wang, *Analytical electrochemistry*, Wiley-VCH, (2000) New York, USA.
37. K. Khachatryan, S. Smirnova, I. Torocheshnikova, N. Shvedene, A. Formanovsky and I. Pletnev, *Anal Bioanal Chem*, 381(2005)464.
38. L. Chu, L. Han and X. Zhang, *J Appl Electrochem*, 41(2011)687.
39. P. Calvo-Marzal, SS. Rosatto, PA. Granjeiro, H. Aoyama and L.T. Kubota, *Anal Chim Acta*, 441(2001)207.
40. Z. Liu, J. Du, C. Qiu, L. Huang, H. Ma, D. Shen and Y. Ding, *Electrochem Comm*, 11(2009)1365.
41. J. Fischer, L. Vanourkova, A. Danhel, V. Vyskocil, K. Cizek, J. Barek, K. Peckova, B. Yosypchuk and T. Navratil, *Int J Electrochem Sci*, 2(2007)226.
42. Z. Liu, X. Ma, H. Zhang, W. Lu, H. Ma and S. Hou, *Electroanalysis*, 24(2012)1178.

© 2016 The Authors. Published by ESG (www.electrochemsci.org). This article is an open access article distributed under the terms and conditions of the Creative Commons Attribution license (<http://creativecommons.org/licenses/by/4.0/>).